Çukurova Üniversitesi Mühendislik Mimarlık Fakültesi Dergisi, 31(ÖS 2), ss. ÖS 175-ÖS 180, Ekim 2016
Çukurova University Journal of the Faculty of Engineering and Architecture, 31(SI 2), pp. SI 175-SI 180, October 2016

Production, Characterization and Effect of Te Doping on FeSe-11 Compounds

Derya FARİSOĞULLARI*[1], Nilay KANTARCI GÜLER[1], Faruk KARADAĞ[1], Ahmet EKİCİBİL[1], Bekir ÖZÇELİK[1]

[1]*Cukurova University, Department of Physics, Faculty of Sciences and Letters, Adana, Turkey*

Geliş tarihi: 01.08.2016 Kabul tarihi: 17.10.2016

Abstract

In this work, $FeTe_{0.7}Se_{0.3}$ single crystals have been synthesized by using the self-flux method, in order to understand effect of Te doping in the Fe-chalcogenides. For this purpose, the physical properties of sample have been investigated by Scanning Electron Microscopy (SEM), Energy dispersive x-ray (EDX) spectroscopy, X-ray diffraction (XRD) and magnetic techniques. The XRD results show that the sample has tetragonal structure, with some impurity peaks. SEM results demonstrate that the sample is distributed in a terrace-like formation. EDX results indicate that the distribution of Fe, Te and Se on the surface of the sample is homogenous. According to χ^{-1}-T measurement, antiferromagnetic interaction is observed. In addition, M-H curves show nearly paramagnetic behavior for the sample measured.

Keywords: Fe-based superconductivity, Self-flux method, XRD, SEM, Magnetism

Te Katkısının FeSe-11 Bileşiklerine Etkisi, Üretimi ve Karakterizasyonu

Öz

Bu çalışma kapsamında, Fe-kalkojenlerin fiziksel mekanizmasını daha iyi irdelemek için $FeTe_{0.7}Se_{0.3}$ tek kristali self-flux metodu kullanılarak sentezlendi. Bu bağlamda, hazırlanan numunenin fiziksel özellikleri, Taramalı Elektron Mikroskopu (SEM), Enerji Saçılımlı X-ışını Spektroskopi (EDX), X-Işını Kırınımı (XRD) ve manyetik teknikleri kullanılarak incelendi. Numune, XRD sonucunda tetragonal kristal yapı ile birlikte bazı safsızlık piklerinin de varlığını sergilemektedir. SEM sonucu, numunenin terasa benzer bir oluşum olduğunu göstermektedir. EDS sonucu, Fe, Te ve Se elementlerinin numune yüzeyinde homojen olarak dağıldığını göstermektedir. χ^{-1}-T ölçümlerine göre, numunede antiferromanyetik etkileşmeler gözlemlenmektedir. Buna ek olarak, M-H grafiklerinde ise neredeyse paramanyetik davranışın olduğunu göstermektedir.

Anahtar Kelimeler: Fe-tabanlı süperiletkenler, Self-flux metodu, XRD, SEM, Manyetizma

---

[*] Sorumlu yazar (Corresponding author): Derya FARİSOĞULLARI, *deryafarisogullari@gmail.com*

1. INTRODUCTION

Superconductivity in mercury was discovered in 1911 by Kamerling Onnes [1], since then it has attracted wordwide attention because superconductors have unique properties such as zero resistance state a desire to lower energy losses. Over the last one-hundered years several researchers have studied this field and they have found that many elements, alloys and ceramics show superconducting properties below defined critical temperatures (T_c) [2]. The greatest leap in 1986 came with, the discovery of a new class of superconducting copper oxides, so-called as high temperature superconductors (HTS), by Bednorz and Muller [3], which now have critical temperatures T_c, of 138 K after doping and up to 164K under pressure [4,5]. In 2008 the scientific world was astonished by the discovery of a thoroughly new class of iron based superconductors. The discovery $LaO_{1-x}F_xFeAs$ superconductors with superconducting transition temperature 26K was reported by Hosono's group [6]. Since then, numerous researchers have provided this new materials a second family of high-Tc superconductors. To date, the parent materials are classified into five types namely: REOFeAs ('1111', RE=rare earth) [6], $AeFe_2As_2$ ('122', Ae=alkaline earth) [7], LiFeAs ('111') [8], Fe(Se,Ch) ('11' Ch=S, Te) [9] and '32225' family of Sr_2MO_3FePn (M=Sc, V, Cr and Pn=pnictogen) [10]. Among the Fe-based superconductors, FeSe-11 so-called chalcogenides have drawn much attention because of their simplest structure and less toxicity compared to the As-based compounds. Morever, tetragonal FeSe which was reported with critical temperature Tc of 8K at ambient pressure, with the substitution of Te with Se, up to 14K in $FeTe_{1-x}Se_x$ compound [11] and up to 37K at hydrostatic pressure [12].

In this work, high-quality $FeTe_{0.7}Se_{0.3}$ single crystal have been produced and their physical properties investigated by Scanning Electron Microscopy (SEM) together with energy dispersive x-ray (EDX) spectroscopy, X-ray diffraction (XRD), magnetization and magnetic hysteresis techniques.

2. MATERIALS AND METHODS

Single crystals with nominal composition $FeTe_{0.7}Se_{0.3}$ were prepared by self-flux method. The granular of Fe (99.99%) and the shot of Se (99.999%) and Te (99.999%) were put into a quartz tube with molar ratio of $FeTe_{0.7}Se_{0.3}$ and sealed under high vacuum. The quartz tube was placed in a second quartz tube for the purpose of cracking the tube during the sintering process. The double quartz tube was heated to 1050^{o}C and maintained at that temperature for 24 hours then slowly cooled down to 700^{o}C at rate of 1.45^{o}C/h. The structure of the sample was characterized by X-ray diffraction (XRD) at room temperature with Cu-Kα radiation (Rigaku D/max-B) and a constant scan rate between $2\theta = 2 - 80^o$. Scanning Electron Microscopy (SEM) were taken using a LEO Evo-40 VPX SEM fitted with energy dispersive X-ray (EDX) analyzer. The magnetic properties were measured by using a physical property measurement system (PPMS, Quantum Design) magnetometer.

3. RESULTS AND DISCUSSION

3.1. X-Ray Characterization

The crystal was found to be very shiny, grown along the ab-plane, and was easy to cleave along this plane. The x-ray diffraction (XRD) pattern of $FeTe_{0.7}Se_{0.3}$ single crystal is shown in figure 1. The high intensity of the (00ℓ) indices from the XRD pattern shows the c-axis orientation of the single crystal. The powder XRD pattern of single crystal, four narrow and sharp peaks appear at about $2\theta \approx 14.83^o$, 29.41^o, 44.47^o, 60.50^o, which correspond to the reflected intensity from the (001), (002), (003), (004) planes of the tetragonal crystal structure with space group of P4/nmm. This result is in good agreement with earlier reports [11]. In addition to this, there exists some impurities at about $2\theta \approx 21.66^o$, 24.02^o, 26.92^o, whose peaks are very weak. A possible explanation that the disappearance of Se or some of the Te is not integrated into the sample attributed to the formation of FeTe/FeSe binary phases. The lattice parameters were calculated and found to be a=3.86559^{o}A, c= 6.02458^{o}A and

V=89.53 A^3 by standard Rietveld refinement method using FullProf software.

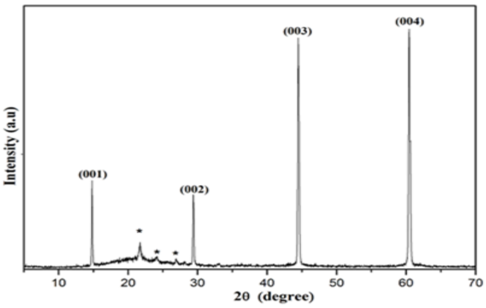

Figure 1. X-ray diffraction pattern of FeTe0.7Se0.3 single crystal

3.2. SEM Analysis

The morphology of the surface and the ratio of Fe:Te:Se was investigated by SEM with energy dispersive X-ray spectrum (EDX). The SEM images 10.000X magnification are given in Figure 2a. As seen the figure, the sample is distributed in a terrace-like formation. Energy dispersive X-ray (EDX) spectra of the sample is given in Figure 2b. It demonstrated that all of the points in the single crystal include the expected elements (Fe, Se, Te) without any trace of impurities. According to the mapping image, for the sample, all of the elemental distribution is almost uniform on the whole area scanned. In addition, the EDX analysis reveals the ratio of the elements in as $Fe_{0.91}Te_{0.39}Se_{0.56}$. These differences between actual chemical composition and nominal chemical composition can be explained that Te is not integrated into the crystal structure of FeSe as confirmed by the x-ray diffraction result.

3.3. Magnetic Properties

DC magnetic properties of Te doped FeSe have been investigated by measuring the magnetization of the sample with a PPMS magnetometer. Firstly, the temperature dependence of field-cooled (FC) magnetization at 20 Oe was measured (see Figure 3), and secondly, magnetization aganist magnetic fields (M-H) at 8 K, 10 K and 12 K temperatures were measured in an applied magnetic field range of -9 T to +9 T (see Figure 4).

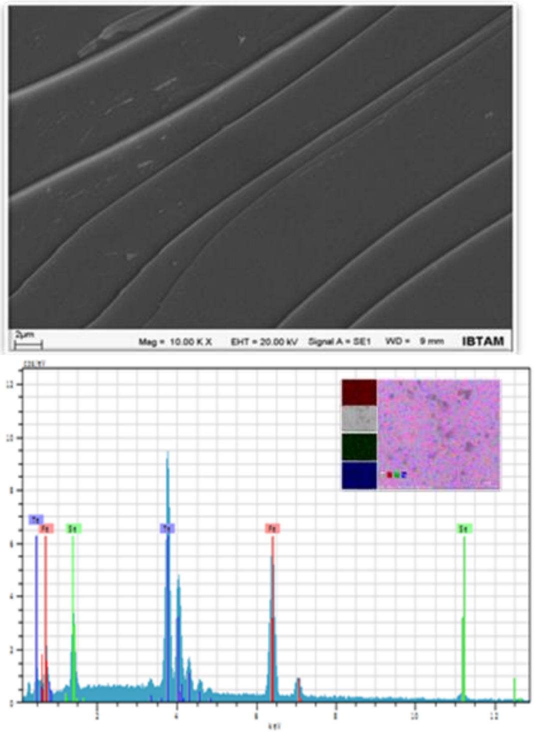

Figure 2. SEM images and EDS spectrums of the $FeTe_{0.7}Se_{0.3}$ single crystal. Inset shows EDS dot maps

According to Figure 3, the DC susceptibility (χ) obtained at 5 K, is the highest and then the DC susceptibility values decreases with an increasing temperature up to 50 K. This reveals that magnetic moments are very sensitive to the temperature.

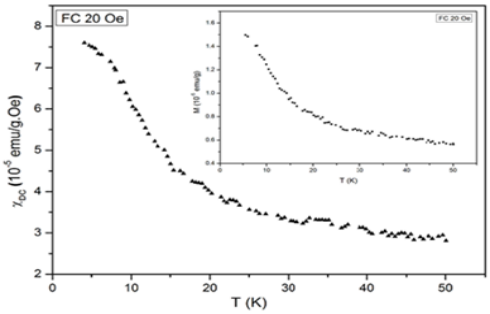

Figure 3. DC-susceptibility curves obtained from the FC magnetizations at 20 Oe for the $FeTe_{0.7}Se_{0.3}$. Inset shows FC magnetizations versus temperature at 20 Oe external field

From Figure 4, it can be seen that, above ±2 T, the curves of M-H are linearly varying with magnetic fields, which signifies that the sample shows paramagnetic behaviour at all temperatures. However, there is a slight hysteresis between ±2 T (given the inset figure 4) for all the temperature. The small amount of impurities may be the reason for the ferromagnetic component in M-H curves.

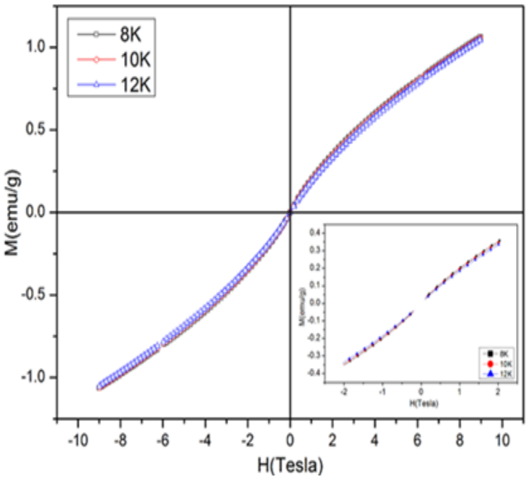

Figure 4. Magnetization against magnetic field curves for $FeTe_{0.7}Se_{0.3}$ at 8 K, 10 K and 12 K

The inverse susceptibility ($1/\chi_{D.C}$) versus temperature curves plotted for the $FeTe_{0.7}Se_{0.3}$ single crystal are given in figure 5. According to the figure, the curves display Curie-Weiss behavior, where it can be expressed using Cruie-Weiss law as follows:

$$1/\chi_{D.C} = H/M = (T-\theta)/C \qquad (1)$$

where C and θ are Curie-Weiss temperature, respectively. The extrapolation of the straight lines, obtained from the data at higher temperatures cut the temperature axis on the negative side which marks the Curie-Weiss temperature, θ. The value of the θ is negative and magnitude of it is not high. This means that their is the substitution of Te with Se, and in addition to the paramagnetic contribution there is also a antiferromagnetic interaction in the sample.

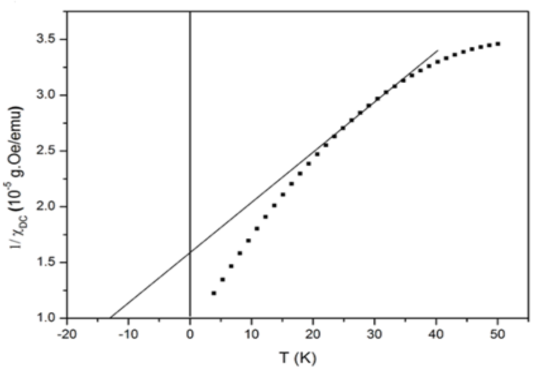

Figure 5. Inverse DC-susceptibility curves for $FeTe_{0.7}Se_{0.3}$

4. CONCLUSION

In conclusion, $FeTe_{0.7}Se_{0.3}$ single crystal were successfully synthesized by using the self-flux technique. The XRD results showed that the sample has a tetragonal structure. SEM results demonstrated that the sample is distributed in a terrace-like formation. EDX results showed that Fe, Te, and Se were evenly distributed throughout the sample. According to M(T) curves obtained in the DC magnetic fields of 20 Oe (χ^{-1}-T) measurements both paramagnetic interaction and antiferromagnetic interaction were observed. In addition, M-H curves were measured at various temperatures with a magnetic field applied parallel to the c-axis. The sample showed nearly paramagnetic behavior at all temperature intervals.

5. ACKNOWLEDGEMENT

This work is supported by Research Fund of Cukurova University, Adana, Turkey, under grant contracts no: FDK-2015-4036 and FBA-2015-4464

6. REFERENCES

1. Onnes, H.K., 1911. The superconductivity of mercury, Commun. Phys. Lab. Univ. Leiden, p. 122–124.
2. Marouchkine, A., 2004. Room-Temperature Superconductivity, Cambridge International Science Publishing, Cambridge, UK, p. 82-93.

3. Bednorz, J.G., Muller, K.A., 1986. Possible High Tc Superconductivity in the Ba-La-Cu-O System, Z. Phys. B vol. 64, p. 189-193.

4. Dai, P., Chakoumakos, B.C., Sun, G.F., Wong, K.W., Xin, Y., Lu, D.F., 1995. Synthesis and Neutron Powder Diffraction Study of the Superconductor $HgBa_2Ca_2Cu_3O_{8+\delta}$ by Tl Substitution, Physica C: Superconductivity. 243, p. 201–206.

5. Monteverdea, M., Núñez-Regueiroa, M., Achab, C., Lokshinc, K.A., Pavlovc, D.A., Putilinc, S.N., Antipovc, E.V., 2004. Fluorinated Hg-1223 under Pressure: the Ultimate Tc of the Cuprates?, Physica C: Superconductivity. 408-410, p. 23-24.

6. Kamihara, Y., Watanabe, T., Hirano, M., Hosono, H., 2008. Iron-based Layered Superconductor $La[O_{1-x}F_x]FeAs$ (x= 0.05-0.12) with Tc=26 K, J. Am. Chem. Soc. 130, p. 3296-3297.

7. Rotter, M., Tegel, M., Johrendt, D., 2008. Superconductivity at 38 K in the Iron Arsenide $(Ba_{1-x}K_x)Fe_2As_2$ Phys. Rev. Lett., 101, p. 1–4.

8. Chu, C.W., Chen, F., Gooch, M., Guloy, A.M., Lorenz, B., Lv, B., Sasmal, K., Tang, Z.J, Tapp, J.H., Xue, Y.Y., 2009. The Synthesis and Characterization of LiFeAs and NaFeAs, Physica C: Superconductivity, 469, p. 326-331.

9. Hsu, F.C., Luo, J.Y., Yeh, K.W., Chen, T.K., Huang, T.W., Wu, P.M., Lee, Y.C., Huang, Y.L., Chu, Y.Y., Yan, D.C., Wu, M.K., 2008. Superconductivity in the PbO-type Structure Alpha-FeSe, Proc. Natl Acad. Sci., 105, p. 14262–14264.

10. Zhu, X., Han, F., Mu, G., Zeng, B., Cheng, P., Shen, B., Wen, H., 2009. $Sr_3Sc_2Fe_2As_2O_5$ as a Possible Parent Compound for FeAs-based Superconductors, Phys. Rev. B 79, 024516.

11. Wu, Z.F., Wang, Z.H., Tao, J., Qiu, L., Yang, S.G., Wen, H.H., 2016. Flux Pinning and Relaxation in $FeSe_{0.5}Te_{0.5}$ Single Crystals, Supercond. Sci. Technol., 29, 035006 (6pp).

12. Medvedev, S., McQueen, T.M., Troyan, I.A., Palasyuk, T., Eremets, M.I., Cava, R.J., Naghavi, S., Casper, F., Ksenofontov, V., Wortmann, G., Felser, C., 2009. Electronic and Magnetic Phase Diagram of Bold Italic Beta-$Fe_{1.01}Se$ with Superconductivity at 36.7 K under Pressure, Nat. Mater., 8, p. 630–633.